

RDS-DeePC: Robust Data Selection for Data-Enabled Predictive Control via Sensitivity Score

Jiachen Li, Shihao Li
 The University of Texas at Austin
 {jiachenli, shihao01301}@utexas.edu

Abstract—Data-Enabled Predictive Control (DeePC) offers a powerful model-free approach to predictive control, but faces two fundamental challenges: computational complexity scaling cubically with dataset size, and severe performance degradation from corrupted data. This paper introduces Robust Data Selection DeePC (RDS-DeePC), which addresses both challenges through influence function analysis. We derive a sensitivity score quantifying each trajectory segment’s leverage on the optimization solution, proving that high-sensitivity segments correspond to outliers while low-sensitivity segments represent consistent data. By selecting low-sensitivity segments, RDS-DeePC achieves computational efficiency and automatic outlier filtering without requiring data quality labels. For nonlinear systems, we extend the framework through a two-stage online selection approach accelerated by the LiSSA algorithm.

Index Terms—Data-driven control, predictive control, influence functions, robust control, outlier detection, data selection, computational efficiency

I. INTRODUCTION

Data-Enabled Predictive Control (DeePC) [1] has emerged as a compelling framework for model-free predictive control. By leveraging Willems’ fundamental lemma [2], DeePC directly uses input-output trajectory data to predict future system behavior without requiring explicit system identification. This behavioral systems approach [3] has demonstrated success across diverse applications including power electronics [4], building climate control [5], autonomous vehicles [6], and robotic systems [7].

Despite its theoretical elegance, practical DeePC deployment faces two fundamental challenges that this paper addresses.

A. Challenge 1: Computational Intractability

The computational complexity of DeePC scales cubically with the number of trajectory segments T in the Hankel matrices. For a dataset with N_d samples and horizon parameters yielding $T = N_d - L + 1$ segments, the optimization problem at each Model Predictive Control (MPC) step requires $O(T^3)$ operations for direct solvers or $O(T^2)$ per iteration for iterative methods. This scaling poses a severe limitation for real-time control, particularly when compared to fast MPC implementations that exploit problem structure [8].

Consider a modest dataset of $N_d = 5000$ samples yielding $T \approx 4000$ segments: direct solution requires approximately 6×10^{10} operations per MPC step, rendering real-time control at typical sampling rates (20–100 Hz) infeasible on standard hardware. As Luppi and Jones [9] emphasize, data selection

is not merely beneficial but *necessary* for online DeePC implementation. The question is not whether to select data, but how to select it intelligently. Naive approaches such as random selection or simple distance-based filtering provide no quality guarantees and may inadvertently include problematic data while excluding valuable segments.

B. Challenge 2: Sensitivity to Data Quality

Real-world trajectory data inevitably contains imperfections arising from sensor noise and measurement errors, actuator faults causing input-output mismatch, data from different operating conditions or system configurations, and corrupted or mislabeled recordings. When such corrupted data enters the Hankel matrices, DeePC performance degrades substantially, often catastrophically.

Existing approaches address data quality through regularization [10] or robust optimization [11]. The learning-based MPC literature [12] has also explored various strategies for handling uncertain data. While these methods improve nominal robustness, they do not explicitly identify and remove problematic data segments. The corrupted data remains in the optimization, continuing to bias the solution even if its effect is partially mitigated.

C. Our Contribution: Solving Both Challenges Simultaneously

This paper introduces Robust Data Selection DeePC (RDS-DeePC), which leverages influence functions from robust statistics [13], [14] to derive a *sensitivity score* measuring each trajectory segment’s leverage on the DeePC optimization solution. Our key insight is that these two challenges can be addressed through a single mechanism: high-sensitivity segments are high-leverage points that disproportionately affect the optimization solution, and when data quality is heterogeneous, these high-leverage points typically correspond to outliers or corrupted data. By selecting low-sensitivity segments, we simultaneously achieve computational reduction and automatic outlier filtering.

The contributions of this paper are threefold. First, we derive the sensitivity score $S(z_j) = 2\lambda_g g_j^* p_j$ using influence function theory [15] and establish its interpretation as a leverage measure that identifies high-influence data points. Second, we develop the RDS-DeePC algorithm for LTI systems that achieves robust control performance even when a significant fraction of data is corrupted, while simultaneously providing dramatic computational speedup. Third, we extend

RDS-DeePC to nonlinear systems through a two-stage online selection framework combining locality-based filtering with sensitivity-based robust selection, accelerated by the LiSSA algorithm [21] for computational efficiency.

Experimental results on DC motor position control demonstrate that RDS-DeePC achieves 99% improvement over random selection when 20% of data is corrupted, while providing over 800 \times computational speedup compared to full-data DeePC.

II. PRELIMINARIES

A. Notation

We denote by \mathbb{R}^n the n -dimensional Euclidean space. For a matrix A , A^\top denotes its transpose, $A(:, j)$ denotes the j -th column, and $\|A\|$ denotes the spectral norm. For a vector v and positive definite matrix P , $\|v\|_P^2 = v^\top P v$ denotes the weighted squared norm. The identity matrix of dimension n is I_n , and e_j denotes the j -th standard basis vector. We use $\text{diag}(\cdot)$ to construct diagonal matrices.

B. System Description

Consider a discrete-time linear time-invariant (LTI) system:

$$x_{k+1} = Ax_k + Bu_k, \quad y_k = Cx_k + Du_k \quad (1)$$

with state $x_k \in \mathbb{R}^n$, input $u_k \in \mathbb{R}^m$, and output $y_k \in \mathbb{R}^p$ at time step k . We assume access to a pre-collected dataset $\mathcal{D} = \{(u_1, y_1), \dots, (u_{N_d}, y_{N_d})\}$ of N_d input-output measurements.

C. Hankel Matrix Construction

Given trajectory data of length N_d , we construct Hankel matrices with depth $L = T_{\text{ini}} + N$, where T_{ini} is the initial trajectory length for implicit state estimation and N is the prediction horizon. The input Hankel matrix is:

$$\mathcal{H}_L(u) = \begin{bmatrix} u_1 & u_2 & \cdots & u_T \\ u_2 & u_3 & \cdots & u_{T+1} \\ \vdots & \vdots & \ddots & \vdots \\ u_L & u_{L+1} & \cdots & u_{N_d} \end{bmatrix} \in \mathbb{R}^{Lm \times T} \quad (2)$$

where $T = N_d - L + 1$ is the number of trajectory segments. The output Hankel matrix $\mathcal{H}_L(y) \in \mathbb{R}^{Lp \times T}$ is constructed analogously.

We partition the Hankel matrices into past and future components:

$$\begin{bmatrix} U_p \\ U_f \end{bmatrix} = \mathcal{H}_L(u), \quad \begin{bmatrix} Y_p \\ Y_f \end{bmatrix} = \mathcal{H}_L(y) \quad (3)$$

where $U_p \in \mathbb{R}^{T_{\text{ini}}m \times T}$, $U_f \in \mathbb{R}^{Nm \times T}$, $Y_p \in \mathbb{R}^{T_{\text{ini}}p \times T}$, and $Y_f \in \mathbb{R}^{Np \times T}$.

Each column $j \in \{1, \dots, T\}$ represents a *trajectory segment*:

$$z_j = [U_p(:, j)^\top \quad U_f(:, j)^\top \quad Y_p(:, j)^\top \quad Y_f(:, j)^\top]^\top \quad (4)$$

corresponding to a length- L window of the original data starting at time index j .

TABLE I: DeePC Computational Scaling with Dataset Size

T (segments)	Operations	Time @ 1 GFLOP/s	Real-time?
100	10^6	1 ms	✓
500	1.25×10^8	125 ms	Marginal
1000	10^9	1 s	✗
4000	6.4×10^{10}	64 s	✗

D. Willems' Fundamental Lemma

The theoretical foundation of DeePC is Willems' fundamental lemma [2], which has seen renewed interest in the data-driven control community [3]:

Lemma 1 (Willems et al., 2005). *Consider an LTI system (1) of order n . If the input sequence $\{u_1, \dots, u_{N_d}\}$ is persistently exciting of order $L + n$, then any valid length- L input-output trajectory (\bar{u}, \bar{y}) of the system can be expressed as:*

$$\begin{bmatrix} U_p \\ Y_p \\ U_f \\ Y_f \end{bmatrix} g = \begin{bmatrix} u_{\text{ini}} \\ y_{\text{ini}} \\ \bar{u} \\ \bar{y} \end{bmatrix} \quad (5)$$

for some coefficient vector $g \in \mathbb{R}^T$.

This lemma enables prediction of future trajectories directly from data, without explicit system identification.

E. Data-Enabled Predictive Control

Based on Lemma 1, DeePC [1] formulates predictive control as a data-driven optimization. In the presence of noise, the regularized formulation [10] solves:

$$\begin{aligned} \min_g \quad & \|Y_f g - y_{\text{ref}}\|_Q^2 + \|U_f g\|_R^2 + \lambda_g \|g\|^2 \\ & + \lambda_y \|Y_p g - y_{\text{ini}}\|^2 + \lambda_u \|U_p g - u_{\text{ini}}\|^2 \end{aligned} \quad (6)$$

where $y_{\text{ref}} \in \mathbb{R}^{Np}$ is the reference trajectory, $Q \succ 0$ and $R \succ 0$ are tracking and control weights, $\lambda_g > 0$ regularizes the coefficient vector, and $\lambda_y, \lambda_u \gg 1$ enforce the initial trajectory constraints. The first control input $u_0 = (U_f g^*)_{1:m}$ is applied in a receding horizon fashion.

F. Computational Complexity of Standard DeePC

The optimization (6) is an unconstrained quadratic program with T decision variables. The normal equations yield:

$$Hg^* = b \quad (7)$$

where $H \in \mathbb{R}^{T \times T}$ is the Hessian and $b \in \mathbb{R}^T$ is the linear term. Direct solution via Cholesky factorization requires $O(T^3)$ operations.

For typical applications with T in the thousands, this computational burden is prohibitive for real-time MPC. Table I illustrates the scaling:

This motivates the need for data selection: using a carefully chosen subset of $K \ll T$ segments reduces complexity to $O(K^3)$, potentially enabling real-time control.

G. Influence Functions Background

Influence functions, originating from robust statistics [13], [14], quantify how individual data points affect statistical estimators. In machine learning, Koh and Liang [15] popularized their use for understanding model predictions, with subsequent work extending the theory [16] and scaling the computation to large models [17], [18].

The core idea is as follows: consider an objective function where sample z 's contribution is scaled by weight w . The influence function measures how the optimal parameters change when w is perturbed, computed via the implicit function theorem without re-optimization. This provides an efficient approximation to leave-one-out analysis. Related approaches for data valuation include Data Shapley [19] and coresets methods [20], though these have different computational tradeoffs.

III. SENSITIVITY SCORE VIA INFLUENCE FUNCTIONS

In this section, we derive a sensitivity score for each trajectory segment using influence function analysis. This score quantifies the leverage of each segment on the DeePC optimization and enables principled data selection.

A. Trajectory-Weighted DeePC Formulation

To analyze individual trajectory contributions, we introduce per-segment weights $w = [w_1, \dots, w_T]^\top \in \mathbb{R}^T$ with $W = \text{diag}(w)$. The weighted DeePC objective becomes:

$$J(g; w) = \|Y_f W g - y_{\text{ref}}\|_Q^2 + \|U_f W g\|_R^2 + \lambda_g \|g\|^2 + \lambda_y \|Y_p W g - y_{\text{ini}}\|^2 + \lambda_u \|U_p W g - u_{\text{ini}}\|^2 \quad (8)$$

At baseline $w_j = 1$ for all j , this recovers standard DeePC (6). The predicted output is $\hat{y} = Y_f W g = \sum_{j=1}^T w_j g_j Y_f(:, j)$, so setting $w_j = 0$ removes segment z_j 's contribution entirely.

Expanding into quadratic form:

$$J(g; w) = g^\top W M W g - 2b^\top W g + \lambda_g \|g\|^2 + \text{const} \quad (9)$$

where:

$$M = Y_f^\top Q Y_f + U_f^\top R U_f + \lambda_y Y_p^\top Y_p + \lambda_u U_p^\top U_p \quad (10)$$

$$b = Y_f^\top Q y_{\text{ref}} + \lambda_y Y_p^\top y_{\text{ini}} + \lambda_u U_p^\top u_{\text{ini}} \quad (11)$$

The Hessian is $\nabla_g^2 J = W M W + \lambda_g I_T$, and at baseline $w = \mathbf{1}$:

$$H = M + \lambda_g I_T \quad (12)$$

The optimality condition is:

$$(W M W + \lambda_g I_T) g^*(w) = W b \quad (13)$$

B. Influence on Optimal Coefficients

We first derive how perturbations to segment weights affect the optimal solution.

Proposition 1 (Influence on Optimal Coefficients). *The influence of trajectory segment z_j on the optimal coefficient vector, evaluated at the baseline $w = \mathbf{1}$, is:*

$$\mathcal{I}_g(z_j) := \frac{dg^*}{dw_j} \Big|_{w=1} = g_j^* H^{-1} (\lambda_g e_j - m_j) \quad (14)$$

where $m_j = M(:, j)$ is the j -th column of M and e_j is the j -th standard basis vector.

Proof. Define the implicit function $F(g, w) = (W M W + \lambda_g I_T)g - W b$, satisfying $F(g^*(w), w) = 0$ at optimality. The partial derivatives are:

$$\frac{\partial F}{\partial g} = W M W + \lambda_g I_T \quad (15)$$

For the weight derivative, using $\frac{\partial W}{\partial w_j} = e_j e_j^\top$:

$$\frac{\partial F}{\partial w_j} = (e_j e_j^\top M W + W M e_j e_j^\top) g - b_j e_j \quad (16)$$

At baseline $w = \mathbf{1}$, this simplifies to:

$$\frac{\partial F}{\partial w_j} \Big|_{w=1} = [M g^*]_j e_j + g_j^* m_j - b_j e_j \quad (17)$$

From the optimality condition $H g^* = b$, we have $M g^* = b - \lambda_g g^*$, so $[M g^*]_j = b_j - \lambda_g g_j^*$. Substituting:

$$\frac{\partial F}{\partial w_j} \Big|_{w=1} = -\lambda_g g_j^* e_j + g_j^* m_j = g_j^* (m_j - \lambda_g e_j) \quad (18)$$

By the implicit function theorem:

$$\frac{dg^*}{dw_j} = - \left(\frac{\partial F}{\partial g} \right)^{-1} \frac{\partial F}{\partial w_j} \quad (19)$$

$$= -H^{-1} \cdot g_j^* (m_j - \lambda_g e_j) \quad (20)$$

$$= g_j^* H^{-1} (\lambda_g e_j - m_j) \quad (21)$$

□

C. Sensitivity Score Derivation

To obtain a scalar measure for data selection, we consider how perturbations affect a test metric. Define the control cost:

$$f(g; w) = \|Y_f W g - y_{\text{ref}}\|_Q^2 + \|U_f W g\|_R^2 \quad (22)$$

which evaluates prediction accuracy and control effort at the current operating point.

Theorem 1 (Sensitivity Score). *The sensitivity of trajectory segment z_j , defined as the total derivative of the control cost with respect to segment weight, is:*

$$\mathcal{S}(z_j) := \frac{df(g^*(w); w)}{dw_j} \Big|_{w=1} = 2\lambda_g g_j^* p_j \quad (23)$$

where $p = H^{-1} v$ and $v = \nabla_g f(g^*; \mathbf{1}) = 2(Y_f^\top Q(Y_f g^* - y_{\text{ref}}) + U_f^\top R U_f g^*)$.

Proof. The total derivative decomposes via the chain rule:

$$\frac{df}{dw_j} = \underbrace{\frac{\partial f}{\partial w_j} \Big|_{g=g^*}}_{\text{direct effect}} + \underbrace{\nabla_g f(g^*)^\top \frac{dg^*}{dw_j}}_{\text{indirect effect}} \quad (24)$$

Direct effect. Let $M_f = Y_f^\top Q Y_f + U_f^\top R U_f$ and $c_f = Y_f^\top Q y_{\text{ref}}$. Then $f(g; w) = g^\top W M_f W g - 2c_f^\top W g + \text{const}$, yielding:

$$\frac{\partial f}{\partial w_j} \Big|_{w=1, g=g^*} = 2g_j^* [M_f g^*]_j - 2(c_f)_j g_j^* = g_j^* v_j \quad (25)$$

where $v = \nabla_g f(g^*) = 2(M_f g^* - c_f)$.

Indirect effect. Let $p = H^{-1}v$. From Proposition 1:

$$v^\top \mathcal{I}_g(z_j) = g_j^* v^\top H^{-1}(\lambda_g e_j - m_j) \quad (26)$$

$$= g_j^* (\lambda_g p_j - p^\top m_j) \quad (27)$$

Using $Mp = Hp - \lambda_g p = v - \lambda_g p$, we have $p^\top m_j = [Mp]_j = v_j - \lambda_g p_j$. Thus:

$$v^\top \mathcal{I}_g(z_j) = g_j^* (\lambda_g p_j - v_j + \lambda_g p_j) = g_j^* (2\lambda_g p_j - v_j) \quad (28)$$

Combined. Adding direct and indirect effects:

$$\mathcal{S}(z_j) = g_j^* v_j + g_j^* (2\lambda_g p_j - v_j) = 2\lambda_g g_j^* p_j \quad (29)$$

□

D. Interpretation: Sensitivity as Leverage

The sensitivity score $\mathcal{S}(z_j) = 2\lambda_g g_j^* p_j$ admits a compelling interpretation as a *leverage measure*. Its magnitude $|\mathcal{S}(z_j)|$ quantifies how much the control cost would change if segment z_j 's weight were perturbed.

This interpretation has profound implications for data quality assessment:

Proposition 2 (High Sensitivity Indicates Outliers). *When the data pool contains heterogeneous quality (mixture of clean and corrupted data), high-sensitivity segments typically correspond to outliers or corrupted data. This occurs because corrupted segments create inconsistencies in the Hankel matrices that conflict with the majority of clean data. To accommodate these inconsistencies while minimizing overall cost, the optimizer assigns larger coefficient magnitudes $|g_j^*|$ to corrupted segments. The inconsistency also manifests as higher propagation factors $|p_j|$, since the corrupted segment pulls the solution away from the consensus of clean data. Both factors contribute to elevated $|\mathcal{S}(z_j)|$ for corrupted data.*

Remark 1 (Connection to Robust Statistics). *This interpretation aligns with classical results in robust statistics [13], [14], [22], where influence functions identify high-leverage observations that unduly affect parameter estimates. Recent work in robust estimation [23] has further developed algorithmic approaches to handle adversarial corruption. In DeePC, trajectory segments play the role of observations, and \mathcal{S} measures their leverage on the control optimization.*

E. Selection Criterion: Low Sensitivity

The preceding analysis motivates our selection criterion:

Definition 1 (Low-Sensitivity Selection). *Given a selection size $K < T$, the active set is:*

$$\mathcal{A} = \{j : |\mathcal{S}(z_j)| \text{ is among the } K \text{ smallest}\} \quad (30)$$

Equivalently, $\mathcal{A} = \text{argmin}_{|S|=K} \sum_{j \in S} |\mathcal{S}(z_j)|$.

This selection achieves three objectives simultaneously: outlier filtering by excluding high-sensitivity segments that are potentially corrupted; representative selection by retaining

Algorithm 1 RDS-DeePC: Offline Phase

Require: Hankel matrices $U_p, U_f, Y_p, Y_f \in \mathbb{R}^{\cdot \times T}$

Require: Parameters $Q, R, \lambda_g, \lambda_y, \lambda_u$; selection size K

Require: Nominal initial conditions $(u_{\text{ini}}, y_{\text{ini}})$, reference y_{ref}

```

1: // Construct system matrices
2:  $M \leftarrow Y_f^\top Q Y_f + U_f^\top R U_f + \lambda_y Y_p^\top Y_p + \lambda_u U_p^\top U_p$ 
3:  $H \leftarrow M + \lambda_g I_T$ 
4:  $b \leftarrow Y_f^\top Q y_{\text{ref}} + \lambda_y Y_p^\top y_{\text{ini}} + \lambda_u U_p^\top u_{\text{ini}}$ 
5: // Solve nominal DeePC
6:  $g^* \leftarrow H^{-1}b$  {Cholesky factorization}
7: // Compute sensitivity scores
8:  $M_f \leftarrow Y_f^\top Q Y_f + U_f^\top R U_f$ 
9:  $c_f \leftarrow Y_f^\top Q y_{\text{ref}}$ 
10:  $v \leftarrow 2(M_f g^* - c_f)$ 
11:  $p \leftarrow H^{-1}v$  {Reuse Cholesky factor}
12: for  $j = 1, \dots, T$  do
13:    $\mathcal{S}(z_j) \leftarrow 2\lambda_g g_j^* p_j$ 
14: end for
15: // Select low-sensitivity segments
16:  $\mathcal{A} \leftarrow \text{argsort}(|\mathcal{S}|)_{1:K}$  {K smallest  $|\mathcal{S}|$ }
17: // Construct reduced matrices
18:  $\tilde{U}_p, \tilde{U}_f, \tilde{Y}_p, \tilde{Y}_f \leftarrow$  columns of  $U_p, U_f, Y_p, Y_f$  indexed by  $\mathcal{A}$ 
19:  $\tilde{H} \leftarrow \tilde{M} + \lambda_g I_K$  where  $\tilde{M}$  uses reduced matrices
20: Compute and store Cholesky factorization of  $\tilde{H}$ 
21: return Reduced matrices, Cholesky factor, active set  $\mathcal{A}$ 

```

low-sensitivity segments that are typical and provide consistent, redundant information about the system; and computational reduction by using $K \ll T$ segments to dramatically reduce optimization complexity.

IV. RDS-DEEPC ALGORITHM FOR LTI SYSTEMS

We now present the complete RDS-DeePC algorithm, consisting of an offline phase for data analysis and selection, followed by an online phase for real-time control.

A. Offline Phase: Sensitivity Analysis and Selection

The offline phase computes sensitivity scores and identifies the active set of trajectory segments.

B. Online Phase: Real-Time Control

The online phase solves the reduced DeePC problem at each MPC step using the precomputed active set.

C. Computational Complexity Analysis

Proposition 3 (Complexity Analysis). *Let T be the total number of trajectory segments and K be the selection size. The computational complexity is $O(T^3)$ for the offline phase (constructing H and solving the nominal problem) plus $O(T)$ for sensitivity computation, and $O(K^2)$ per MPC step for the online phase (solving the reduced problem using the precomputed Cholesky factor). The online speedup factor compared to full DeePC is $(T/K)^2$ for iterative solvers or $(T/K)^3$ for direct solvers.*

Algorithm 2 RDS-DeePC: Online Phase

Require: Reduced matrices $\tilde{U}_p, \tilde{U}_f, \tilde{Y}_p, \tilde{Y}_f \in \mathbb{R}^{r \times K}$
Require: Precomputed Cholesky factor of \tilde{H}
Require: Parameters $Q, R, \lambda_g, \lambda_y, \lambda_u$

- 1: **for** each time step $t = 0, 1, 2, \dots$ **do**
- 2: Measure current state, construct $(u_{\text{ini}}, y_{\text{ini}})$
- 3: Obtain reference trajectory y_{ref}
- 4: **// Compute reduced linear term**
- 5: $\tilde{b} \leftarrow \tilde{Y}_f^\top Q y_{\text{ref}} + \lambda_y \tilde{Y}_p^\top y_{\text{ini}} + \lambda_u \tilde{U}_p^\top u_{\text{ini}}$
- 6: **// Solve reduced QP**
- 7: $\tilde{g}^* \leftarrow \tilde{H}^{-1} \tilde{b}$ {Using stored Cholesky factor}
- 8: **// Extract and apply control**
- 9: $u_t \leftarrow (\tilde{U}_f \tilde{g}^*)_{1:m}$
- 10: Apply u_t to system
- 11: **end for**

D. Selection Size Guidelines

The selection size K balances robustness against information loss. Values that are too small ($K < 20$) provide insufficient data for accurate prediction and may exclude some useful information, while values that are too large ($K > 100$) may include some outliers and reduce the computational benefit. A recommended range of $K \in [30, 100]$ typically provides robust performance with significant speedup. A practical heuristic is $K \approx 5\text{--}10 \times$ the effective system order, ensuring sufficient degrees of freedom for prediction while maintaining aggressive data reduction.

V. EXTENSION TO NONLINEAR SYSTEMS

While the RDS-DeePC algorithm in Section IV assumes LTI systems, many practical applications involve nonlinear dynamics. This section extends RDS-DeePC to nonlinear systems through a two-stage online selection framework. Related approaches for nonlinear data-driven control include Koopman-based methods [25] and neural network MPC [7].

A. Challenges for Nonlinear Systems

For a nonlinear system $\dot{x} = f(x, u)$, Willems' fundamental lemma does not hold globally. However, around a given operating trajectory, the system behaves approximately linearly. This motivates two key observations. First, regarding local relevance, data from distant operating regions may be inconsistent with local dynamics and should be excluded. Second, regarding dynamic sensitivity, the sensitivity score depends on the current operating point and must be recomputed online.

The sensitivity score naturally captures both data corruption and operating region mismatch. Data segments from different operating regions create inconsistencies similar to corrupted data, resulting in elevated sensitivity scores. Thus, selecting low-sensitivity data from a locally relevant subset achieves both goals: ensuring consistency with local linearization and filtering corrupted segments.

B. Two-Stage Selection Framework

We propose a two-stage framework that first filters by locality, then applies robust selection within the local subset.

Stage 1: Locality-Based Filtering. Given the current initial trajectory $(u_{\text{ini}}, y_{\text{ini}})$, define a distance metric measuring relevance to the current operating point:

$$d(z_j, z_t) = \left\| \begin{bmatrix} Y_p(:, j) \\ U_p(:, j) \end{bmatrix} - \begin{bmatrix} y_{\text{ini}} \\ u_{\text{ini}} \end{bmatrix} \right\|_W \quad (31)$$

where $W \succ 0$ is a weighting matrix. The local subset \mathcal{L}_t contains the K_L closest segments:

$$\mathcal{L}_t = \text{argsort}(d(\cdot, z_t))_{1:K_L} \quad (32)$$

Stage 2: Sensitivity-Based Robust Selection. Within \mathcal{L}_t , compute local sensitivity scores using the local Hankel matrices and select the K_R segments with lowest sensitivity:

$$\mathcal{A}_t = \left\{ j \in \mathcal{L}_t : |\mathcal{S}^{(\mathcal{L}_t)}(z_j)| \text{ among } K_R \text{ smallest} \right\} \quad (33)$$

where $\mathcal{S}^{(\mathcal{L}_t)}$ denotes sensitivity computed using only columns in \mathcal{L}_t .

C. Efficient Computation via LiSSA

Computing sensitivity scores requires solving $p = H^{-1}v$, which costs $O(K_L^3)$ via direct methods. For online implementation at each MPC step, this may be prohibitive. We employ the Linear time Stochastic Second-order Algorithm (LiSSA) [21] for efficient approximation. Recent work has developed alternative efficient influence computation methods [24], though LiSSA remains well-suited for our setting.

LiSSA exploits the Neumann series expansion:

$$H^{-1} = \sum_{i=0}^{\infty} (I - \alpha H)^i \cdot \alpha \quad (34)$$

which converges when the spectral radius $\rho(I - \alpha H) < 1$, satisfied for $0 < \alpha < 2/\lambda_{\max}(H)$.

The LiSSA iteration is:

$$\tilde{p}^{(i+1)} = v + (I - \alpha H)\tilde{p}^{(i)}, \quad \tilde{p}^{(0)} = v \quad (35)$$

After r iterations, $\tilde{p} \approx \alpha \tilde{p}^{(r)}$ approximates $H^{-1}v$. Averaging over s independent runs reduces variance.

Proposition 4 (LiSSA Complexity). *LiSSA requires $O(K_L \cdot r \cdot s)$ operations to approximate $H^{-1}v$, where r is recursion depth and s is sample count. For typical values $r = 50$, $s = 5$, this significantly outperforms direct $O(K_L^3)$ inversion when $K_L > 250$.*

A practical choice for the scale parameter is:

$$\alpha = \frac{1}{\text{tr}(H)/K_L + \lambda_g} \quad (36)$$

which approximates $1/\bar{\lambda}$ where $\bar{\lambda}$ is the average eigenvalue.

D. Online RDS-DeePC Algorithm

Algorithm 3 presents the complete online procedure.

Algorithm 3 Online RDS-DeePC for Nonlinear Systems

```

Require: Data pool  $\{z_1, \dots, z_T\}$ ; parameters
 $Q, R, \lambda_g, \lambda_y, \lambda_u$ 
Require: Selection sizes  $K_L$  (local),  $K_R$  (robust); LiSSA
parameters  $\alpha, r, s$ 
1: for each time step  $t$  do
2:   // Stage 1: Locality-based filtering
3:   Measure current  $(u_{\text{ini}}, y_{\text{ini}})$ 
4:   for  $j = 1, \dots, T$  do
5:      $d_j \leftarrow d(z_j, z_t)$  via (31)
6:   end for
7:    $\mathcal{L}_t \leftarrow \text{argsort}(d)_{1:K_L}$ 
8:   // Stage 2: Sensitivity-based robust selection
9:   Construct local matrices from  $\mathcal{L}_t$ 
10:  Build  $H_L$ , solve  $g_L^* = H_L^{-1}b_L$ 
11:  Compute  $v_L = 2(M_L g_L^* - c_L)$ 
12:  Approximate  $p_L \approx H_L^{-1}v_L$  via LiSSA (35)
13:  for  $j \in \mathcal{L}_t$  do
14:     $\mathcal{S}_j \leftarrow 2\lambda_g(g_L^*)_j(p_L)_j$ 
15:  end for
16:   $\mathcal{A}_t \leftarrow \text{argsort}(|\mathcal{S}|)_{1:K_R}$  within  $\mathcal{L}_t$ 
17:  // Solve reduced DeePC
18:  Construct reduced matrices from  $\mathcal{A}_t$ 
19:   $\tilde{g}^* \leftarrow \tilde{H}^{-1}\tilde{b}$ 
20:  Apply  $u_t \leftarrow (\tilde{U}_f \tilde{g}^*)_{1:m}$ 
21: end for

```

E. Computational Complexity

Proposition 5 (Online Complexity). *The per-step complexity of Algorithm 3 is:*

$$O(T) + O(K_L \cdot r \cdot s) + O(K_R^2) \quad (37)$$

comprising $O(T)$ for distance computation, $O(K_L \cdot r \cdot s)$ for LiSSA-based sensitivity, and $O(K_R^2)$ for the reduced DeePC solve.

For typical parameters ($T = 4050$, $K_L = 200$, $K_R = 30$, $r = 50$, $s = 5$), the dominant cost is LiSSA at approximately 50,000 operations per step—tractable for real-time control at sampling rates up to several hundred Hertz.

VI. EXPERIMENTAL RESULTS

We evaluate RDS-DeePC on a DC motor (LTI) and inverted pendulum (nonlinear) with 20% corrupted data.

A. DC Motor Position Control

Consider a DC motor with dynamics $J\dot{\omega} = K_t i_a - b\omega$, $L_a \dot{i}_a = V_a - R_a i_a - K_e \omega$, discretized at 50 ms. We collect 50 trajectories ($T = 4050$ segments), with 20% corrupted via high noise ($15 \times$ nominal), sensor bias (± 0.5 rad), and input-output mismatch.

Table II shows Full DeePC degrades from MSE 0.079 to 0.796 rad² with corruption. Random selection fails with high variance (MSE 13.93 ± 23.77 at $K = 30$). RDS-DeePC achieves clean-data performance across all K , automatically

TABLE II: DC Motor Performance with 20% Corrupted Data

Method	K	MSE [rad ²]	RMSE [°]	Clean/ K
Clean-only	4050	0.0790	16.10	all
Full (w/ corrupt)	4050	0.7955	51.10	3240/4050
RDS-DeePC	30	0.0790	16.10	29/30
RDS-DeePC	60	0.0791	16.12	56/60
RDS-DeePC	90	0.0790	16.11	84/90
Random	30	13.93 ± 23.77	213.87	~23/30
Random	60	13.25 ± 6.94	208.52	~47/60
Random	90	6.93 ± 4.67	150.78	~71/90

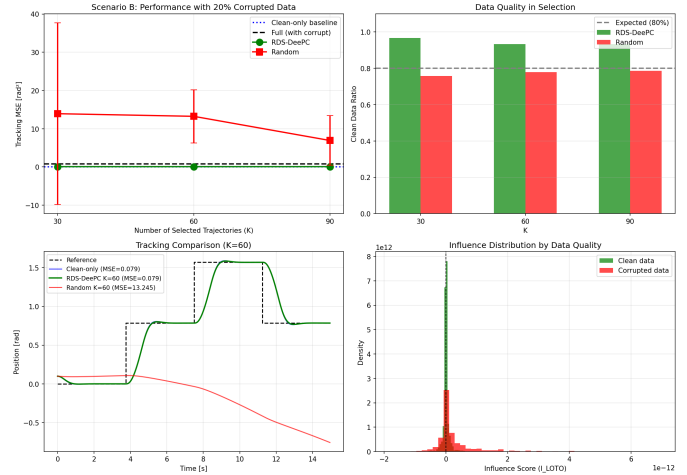


Fig. 1: DC motor with 20% corrupted data. Top-left: MSE comparison. Top-right: Clean data ratio (RDS-DeePC: 93–97% vs. expected 80%). Bottom-left: Tracking at $K = 60$. Bottom-right: Influence score separation.

selecting 93–97% clean segments (Figure 1). Improvement over random: 99.4%.

B. Inverted Pendulum (Nonlinear)

For nonlinear validation, we consider cart-pole stabilization from $\theta_0 = 30^\circ$ to upright. The dynamics are $(m_c + m_p)\ddot{x}_c + m_p l \ddot{\theta} \cos \theta = F + m_p l \dot{\theta}^2 \sin \theta$ with $m_c = 1$ kg, $m_p = 0.1$ kg, $l = 0.5$ m. We collect 100 trajectories with 20% corrupted, using $K_L = 200$ for locality filtering and $K_R = 30$ for sensitivity selection.

Figure 2 and Table III show RDS-DeePC achieves fastest settling (2.1 s vs. 3.5 s for Distance-only—67% faster). Distance-based selection stabilizes but with larger oscillations, demonstrating that sensitivity-based filtering provides value even within locally relevant data. Random selection fails to stabilize, with $|\theta| > 40^\circ$.

VII. CONCLUSION

This paper introduced RDS-DeePC, a robust data selection framework for Data-Enabled Predictive Control that addresses computational intractability and sensitivity to data quality through influence function analysis. The key contribution is the sensitivity score $\mathcal{S}(z_j) = 2\lambda_g g_j^* p_j$, which identifies high-leverage outliers while retaining consistent, low-sensitivity

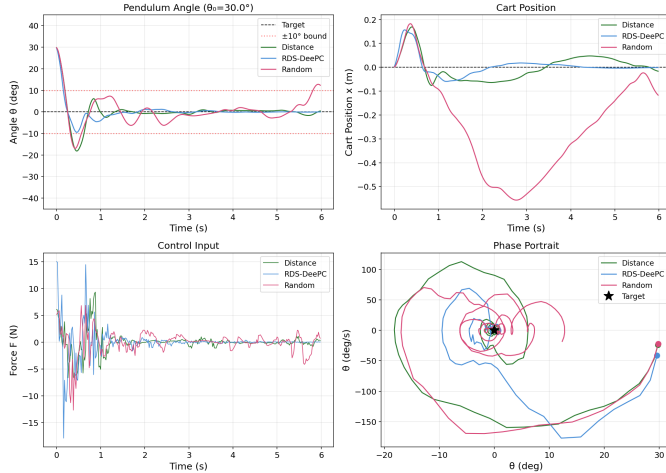


Fig. 2: Inverted pendulum ($\theta_0 = 30^\circ$, 20% corrupted). Top-left: RDS-DeePC stabilizes within $\pm 10^\circ$; Random fails. Top-right: Cart position. Bottom-left: Control input. Bottom-right: Phase portrait.

TABLE III: Inverted Pendulum: Stabilization Metrics

Method	Settling [s]	Max $ \theta $ [$^\circ$]	Final $ x_c $ [m]
RDS-DeePC	2.1	30.0	0.02
Distance	3.5	30.0	0.05
Random	> 6	> 40	> 0.5

data. Experiments on DC motor position control demonstrate big improvement over random selection with 20% corrupted data. The nonlinear extension, validated on inverted pendulum swing-up control, combines locality-based filtering with sensitivity-based selection. By solving both computational and robustness challenges through a single principled mechanism, RDS-DeePC transforms data selection from a practical necessity into a robustness advantage. Future work will explore adaptive selection size determination, theoretical performance guarantees, constrained MPC extensions, and extending the sensitivity measure from the optimization problem to closed-loop control performance (analogous to the original influence function formulation in machine learning).

REFERENCES

- J. Coulson, J. Lygeros, and F. Dörfler, “Data-enabled predictive control: In the shallows of the DeePC,” in *18th European Control Conference (ECC)*, pp. 307–312, IEEE, 2019.
- J. C. Willems, P. Rapisarda, I. Markovsky, and B. L. M. De Moor, “A note on persistency of excitation,” *Systems & Control Letters*, vol. 54, no. 4, pp. 325–329, 2005.
- I. Markovsky and F. Dörfler, “Behavioral systems theory in data-driven analysis, signal processing, and control,” *Annual Reviews in Control*, vol. 52, pp. 42–64, 2021.
- L. Huang, J. Coulson, J. Lygeros, and F. Dörfler, “Data-enabled predictive control for grid-connected power converters,” in *IEEE Conference on Decision and Control*, pp. 8130–8135, 2019.
- Y. Lian, J. Shi, M. Koch, and C. N. Jones, “Adaptive robust data-driven building control via bilevel reformulation: An experimental result,” *IEEE Trans. Control Systems Technology*, vol. 31, no. 6, pp. 2420–2436, 2023.
- E. Elokda, J. Coulson, P. N. Beuchat, J. Lygeros, and F. Dörfler, “Data-enabled predictive control for quadcopters,” *Int. J. Robust and Nonlinear Control*, vol. 31, no. 18, pp. 8916–8936, 2021.
- T. Salzmann, E. Kaufmann, J. Arrizabalaga, M. Pavone, D. Scaramuzza, and M. Ryll, “Real-time neural-MPC: Deep learning model predictive control for quadrotors and agile robotic platforms,” *IEEE Robotics and Automation Letters*, vol. 8, no. 4, pp. 2397–2404, 2023.
- Y. Wang and S. Boyd, “Fast model predictive control using online optimization,” *IEEE Trans. Control Systems Technology*, vol. 18, no. 2, pp. 267–278, 2010.
- A. Luppi and C. N. Jones, “Choose wisely: Data-enabled predictive control for nonlinear systems using online data selection,” *arXiv preprint arXiv:2401.12126*, 2024.
- J. Coulson, J. Lygeros, and F. Dörfler, “Regularized and distributionally robust data-enabled predictive control,” in *IEEE Conference on Decision and Control*, pp. 2696–2701, 2019.
- J. Berberich, J. Köhler, M. A. Müller, and F. Allgöwer, “Data-driven model predictive control with stability and robustness guarantees,” *IEEE Trans. Automatic Control*, vol. 66, no. 4, pp. 1702–1717, 2021.
- L. Hewing, K. P. Wabersich, M. Menner, and M. N. Zeilinger, “Learning-based model predictive control: Toward safe learning in control,” *Annual Review of Control, Robotics, and Autonomous Systems*, vol. 3, pp. 269–296, 2020.
- F. R. Hampel, “The influence curve and its role in robust estimation,” *J. American Statistical Association*, vol. 69, no. 346, pp. 383–393, 1974.
- R. D. Cook and S. Weisberg, “Characterizations of an empirical influence function for detecting influential cases in regression,” *Technometrics*, vol. 22, no. 4, pp. 495–508, 1980.
- P. W. Koh and P. Liang, “Understanding black-box predictions via influence functions,” in *Proc. 34th Int. Conf. Machine Learning (ICML)*, PMLR 70:1885–1894, 2017.
- J. Bae, N. Ng, A. Lo, M. Ghassemi, and R. Grosse, “If influence functions are the answer, then what is the question?” in *Advances in Neural Information Processing Systems (NeurIPS)*, 2022.
- A. Schioppa, P. Zablotckaia, D. Vilar, and A. Sokolov, “Scaling up influence functions,” in *Proc. AAAI Conf. Artificial Intelligence*, vol. 36, no. 8, pp. 8179–8186, 2022.
- R. Grosse, J. Bae, C. Anil, et al., “Studying large language model generalization with influence functions,” *arXiv preprint arXiv:2308.03296*, 2023.
- A. Ghorbani and J. Zou, “Data Shapley: Equitable valuation of data for machine learning,” in *Proc. 36th Int. Conf. Machine Learning (ICML)*, PMLR 97:2242–2251, 2019.
- B. Mirzasoleiman, J. Bilmes, and J. Leskovec, “Coresets for data-efficient training of machine learning models,” in *Proc. 37th Int. Conf. Machine Learning (ICML)*, PMLR 119:6950–6960, 2020.
- N. Agarwal, B. Bullins, and E. Hazan, “Second-order stochastic optimization for machine learning in linear time,” *J. Machine Learning Research*, vol. 18, no. 116, pp. 1–40, 2017.
- X. Pan and W.-X. Zhou, “A new perspective on robust M-estimation: Finite sample theory and applications,” *The Annals of Statistics*, vol. 46, no. 5, pp. 1904–1931, 2018.
- S. B. Hopkins and J. Li, “Robust and heavy-tailed mean estimation made simple, via regret minimization,” in *Advances in Neural Information Processing Systems (NeurIPS)*, 2020.
- Y. Kwon, E. Wu, K. Wu, and J. Zou, “DataInf: Efficiently estimating data influence in LoRA-tuned LLMs and diffusion models,” in *Int. Conf. Learning Representations (ICLR)*, 2024.
- M. Korda and I. Mezić, “Linear predictors for nonlinear dynamical systems: Koopman operator meets model predictive control,” *Automatica*, vol. 93, pp. 149–160, 2018.
- U. Rosolia, X. Zhang, and F. Borrelli, “Data-driven predictive control for autonomous systems,” *Annual Review of Control, Robotics, and Autonomous Systems*, vol. 1, pp. 259–286, 2018.
- C. Verhoek, R. Tóth, and S. Haesaert, “Direct data-driven LPV control of nonlinear systems: An experimental result,” in *IFAC World Congress*, pp. 5263–5268, 2023.
- A. Bemporad and M. Morari, “Robust model predictive control: A survey,” in *Robustness in Identification and Control*, Lecture Notes in Control and Information Sciences, vol. 245, Springer, pp. 207–226, 1999.

APPENDIX

We provide complete derivation details for the sensitivity score.

A. Setup

The weighted test metric is:

$$f(g; w) = \|Y_f W g - y_{\text{ref}}\|_Q^2 + \|U_f W g\|_R^2 \quad (38)$$

Define:

$$M_f = Y_f^\top Q Y_f + U_f^\top R U_f \quad (39)$$

$$c_f = Y_f^\top Q y_{\text{ref}} \quad (40)$$

Then $f(g; w) = g^\top W M_f W g - 2c_f^\top W g + \text{const.}$

B. Direct Effect Computation

At baseline $w = \mathbf{1}$:

$$\frac{\partial f}{\partial w_j} \Big|_{w=\mathbf{1}} = \frac{\partial}{\partial w_j} (g^\top W M_f W g - 2c_f^\top W g) \quad (41)$$

$$= 2g_j[M_f g]_j - 2(c_f)_j g_j \quad (42)$$

At $g = g^*$:

$$\frac{\partial f}{\partial w_j} \Big|_{w=\mathbf{1}, g=g^*} = g_j^* (2[M_f g^*]_j - 2(c_f)_j) = g_j^* v_j \quad (43)$$

where $v = 2(M_f g^* - c_f) = \nabla_g f(g^*; \mathbf{1})$.

C. Indirect Effect Computation

From Proposition 1:

$$\frac{dg^*}{dw_j} = g_j^* H^{-1}(\lambda_g e_j - m_j) \quad (44)$$

Let $p = H^{-1}v$. The indirect effect is:

$$v^\top \frac{dg^*}{dw_j} = g_j^* v^\top H^{-1}(\lambda_g e_j - m_j) \quad (45)$$

$$= g_j^* (\lambda_g p_j - p^\top m_j) \quad (46)$$

Using $Hp = v$ and $H = M + \lambda_g I$:

$$Mp = (H - \lambda_g I)p = v - \lambda_g p \quad (47)$$

Therefore $[Mp]_j = v_j - \lambda_g p_j$, and:

$$p^\top m_j = [Mp]_j = v_j - \lambda_g p_j \quad (48)$$

Substituting:

$$v^\top \frac{dg^*}{dw_j} = g_j^* (\lambda_g p_j - v_j + \lambda_g p_j) \quad (49)$$

$$= g_j^* (2\lambda_g p_j - v_j) \quad (50)$$

D. Combined Result

Adding direct and indirect effects:

$$\mathcal{S}(z_j) = g_j^* v_j + g_j^* (2\lambda_g p_j - v_j) \quad (51)$$

$$= 2\lambda_g g_j^* p_j \quad (52)$$

This completes the proof. \blacksquare

Proposition 6 (LiSSA Convergence). *Let $\kappa = \lambda_{\max}(H)/\lambda_{\min}(H)$ be the condition number. With scale $\alpha = 1/\lambda_{\max}(H)$, after r iterations:*

$$\|\tilde{p}^{(r)} - H^{-1}v\| \leq \left(1 - \frac{1}{\kappa}\right)^r \|H^{-1}v\| \quad (53)$$

Proof. The iteration $\tilde{p}^{(i+1)} = v + (I - \alpha H)\tilde{p}^{(i)}$ with fixed point $p^* = H^{-1}v$ satisfies:

$$\tilde{p}^{(i+1)} - p^* = (I - \alpha H)(\tilde{p}^{(i)} - p^*) \quad (54)$$

The spectral radius of $I - \alpha H$ with $\alpha = 1/\lambda_{\max}(H)$ is:

$$\rho(I - \alpha H) = 1 - \frac{\lambda_{\min}(H)}{\lambda_{\max}(H)} = 1 - \frac{1}{\kappa} \quad (55)$$

By contraction:

$$\|\tilde{p}^{(r)} - p^*\| \leq \left(1 - \frac{1}{\kappa}\right)^r \|\tilde{p}^{(0)} - p^*\| \quad (56)$$

With $\tilde{p}^{(0)} = v$ and $\|v - p^*\| \leq \|v\| + \|p^*\| \leq (1 + \|H^{-1}\|)\|v\|$, the result follows. \square

For DeePC with regularization $\lambda_g > 0$, the Hessian $H = M + \lambda_g I$ is well-conditioned, ensuring rapid convergence.